Available online at www.sciencedirect.com
SCIENCE DIRECT®
Bioorganic & Medicinal Chemistry 12 (2004) 2639–2644
Bioorganic & Medicinal Chemistry

3D-QSAR analysis of conformationally constrained diacylglycerol (DAG) analogues as potent protein kinase C (PK-C) ligands

Su Yeon Kim and Jeewoo Lee*

Laboratory of Medicinal Chemistry, Research Institute of Pharmaceutical Sciences, College of Pharmacy, Seoul National University, Shinlim-Dong, Kwanak-Ku, Seoul 151-742, Republic of Korea

Received 12 January 2004; revised 9 March 2004; accepted 9 March 2004

Available online 2 April 2004

Abstract—A study of the quantitative structure activity relationships (QSARs) was performed based on the binding affinity (pK_i) values of 32 protein kinase C (PK-C) ligands. The QSAR study was carried out by using both three-dimensional descriptors (the steric and electrostatic CoMFA fields) and the physicochemical properties ($\log P$ values). The CoMFA analysis provided a reasonable QSAR model, with a cross-validated q^2 value of 0.671 and a conventional r^2 value of 0.956, which was confirmed by the satisfactory prediction of the experimental binding affinity (pK_i) values for a series of 3-alkylidene-5,5-disubstituted tetrahydro-2-furanones included in the test set. The resultant QSAR model will be useful for designing highly potent and selective PK-C ligands.

1. Introduction

Protein kinase C (PK-C), identified in 1977 by Nishizuka and colleagues,[1,2] is a family of serine/threonine specific isozymes. PK-C has been extensively studied as a pivotal enzyme in cellular signal transduction,[3] and is involved in cell growth, differentiation, apoptosis, and carcinogenesis.[4–7] PK-C is activated by both the second-messenger, diacylglycerol (DAG), and tumor promoters, such as phorbol esters. DAG is generated either by the phospholipase C (PLC)-mediated hydrolysis of phosphatidylinositol-4,5-bisphosphate (PIP_2) or indirectly by phospholipase D and phosphatidic acid hydrolase.[8] DAG induces the translocation of cytosolic PK-C to the inner leaflet of the cellular membrane. There it activates both the calcium-dependent, classical PK-C isoforms (α, β, and γ), and the novel, calcium-independent PK-C isozymes (δ, ε, η, and θ), by binding to the C1 domains of the enzymes and promoting their association with the membrane phospholipids.[9]

The transiently generated DAG is less potent of an endogenous activator than phorbol esters, by a factor of >1000.[10] Since both DAG and phorbol 12,13 dibutyrate (PDBU) bind to the same binding site, the C1 domains of PK-C, in a competitive manner,[11] phorbol esters are powerful pharmacological tools for studying PK-C function. The activation by phorbol esters can persist for a long time due to their metabolic stability, because the conformationally rigid scaffold, unlike the flexible glycerol backbone of DAG, can specifically direct the hydrophilic pharmacophores.

Over the past several years, we have attempted to bridge the affinity gap between phorbol esters and DAGs by two independent, but mutually complementary, approaches.[12,13] The first approach, the pharmacophore-guided approach, seeks to reduce the entropic penalty associated with DAG binding by constraining the glycerol backbone into five-member DAG–lactones. The second approach, the receptor-guided approach, involves the use of highly branched alkyl chains to improve the interaction of the DAG–lactone ligand with a cluster of conserved hydrophobic amino acids (Met239, Pro241, Phe243, Leu250, Trp252, and Leu254) residing between the two β-sheets of the PK-Cδ C1b domain. Using these approaches, we recently obtained an ideal set of branched acyl and 3-alkylidene chains in DAG–lactones with high binding affinities (K_i = 2.3 nM).[14] The increase in the binding affinity by the

Keywords: Three-dimensional quantitative structure activity relationship (3D-QSAR); Comparative molecular field analysis (CoMFA); Protein kinase C (PK-C) ligands.
* Corresponding author. Tel.: +82-2-880-7846; fax: +82-2-888-0649; e-mail: jeewoo@snu.ac.kr

0968-0896/$ - see front matter © 2004 Elsevier Ltd. All rights reserved.
doi:10.1016/j.bmc.2004.03.016

branched alkyl chains is probably due to a combination of two factors: adequate membrane partitioning and specific hydrophobic contacts with the protein.

The correlation between the PK-C binding affinity, pK_i [$= \log(1/K_i)$], and the octanol–water partition coefficient ($\log P$) for a set of DAG–lactones with a combination of linear or branched acyl and 3-alkylidene chains was described previously.[14] The analyzes indicated that the binding affinities of the branched 3-alkylidene and acyl series are maximized at ca. $\log P = 6$ and ca. $\log P = 5$, respectively. From the parabolic dependence between pK_i and $\log P$, it can be concluded that an optimal $\log P$ for these DAG–lactones lies between 5 and 6.

We performed a three-dimensional quantitative structure activity relationship (3D-QSAR) analysis, based on the structural and physicochemical descriptors from comparative molecular field analysis (CoMFA) and $\log P$, to clarify the correlation of the binding affinity and the CoMFA interaction energies with the $\log P$ values. The ultimate purpose of this research is to construct a robust QSAR model to facilitate the identification of compounds with potent binding affinities for PK-C.

2. Results and discussion

The statistical results of the CoMFA analysis are summarized in Table 1. The resulting QSAR model shows good correlation between the experimental and predicted values for a set of DAG–lactones with a combination of linear or branched acyl and 3-alkylidene chains (cross-validated $q^2 = 0.671$, optimum number of components = 5, and conventional $r^2 = 0.956$). The maximum number of components recommended for a partial least square (PLS) analysis is about four or five compounds per component.[15] In this study, an appropriate optimum number of components was obtained with the 26 DAG–lactone derivatives included in the training set.

Table 1. Statistical results of the CoMFA analysis

Cross-validated q^2	0.671
Standard error of prediction	0.699
Optimum number of components	5
Conventional r^2	0.956
Standard error of estimate	0.255
Predictive r^2	0.885
F value	87.894
Relative contributions of parameters	
CoMFA steric	0.453
CoMFA electrostatic	0.383
Log*P* (KowWin)	0.164

Structure activity relationship studies of the DAG–lactones revealed that the highly branched alkyl chains in the compounds enhanced the receptor binding potency by interacting with the hydrophobic amino acids in the binding pocket of the PK-C C1 domains. To acquire more information about the role of the hydrophobic alkyl chains, the $\log P$ (octanol–water partition coefficient) values were calculated and correlated with the binding affinities (pK_i's). In the cases of the branched (**1**–**8**, **13**–**16**, **22**, **29**–**32**) and linear (**9**–**12**, **20**, **21**, **23**–**25**) 3-alkylidene series, the binding affinities are proportional to the $\log P$ values as shown in Figure 1a and b, respectively. The correlation coefficients (r^2) of the branched and linear 3-alkylidene series were measured to be 0.91 and 0.60, respectively. The $\log P$ values of branched 3-alkylidenes are better correlated with the pK_i values than those of linear 3-alkylidenes. However, the binding affinities of the remaining compounds (**17**–**19**,

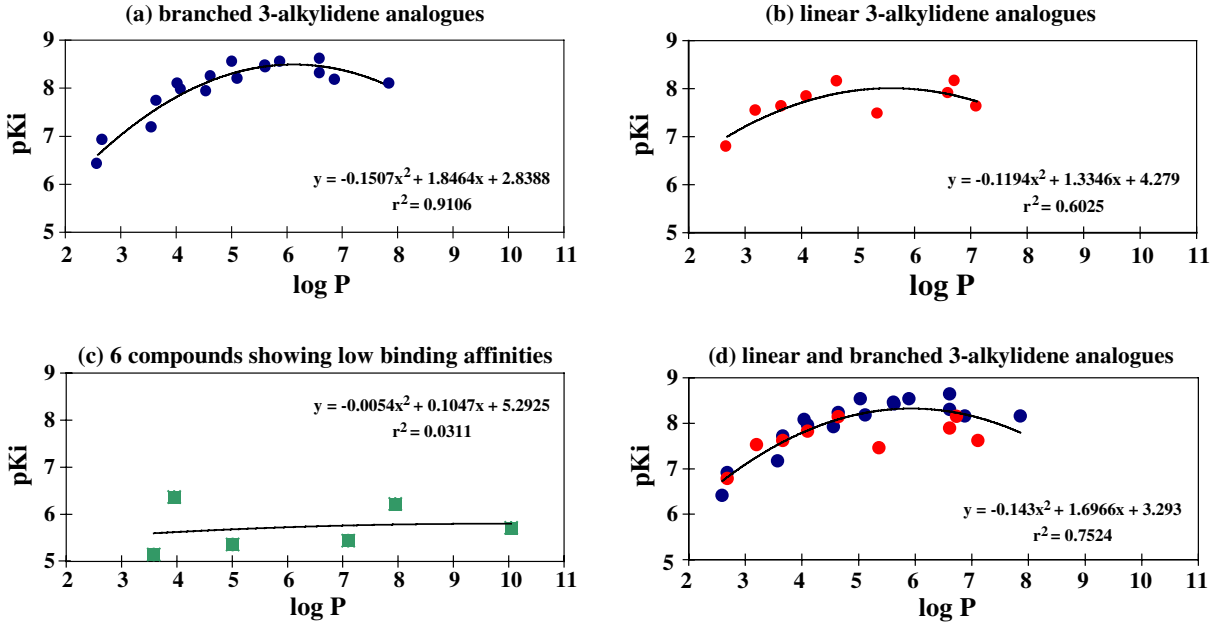

Figure 1. Correlation between binding affinity (pK_i) and $\log P$ values of 32 DAG–lactone derivatives.

26–28) are not correlated with the log*P* values ($r^2 = 0.031$) as represented in Figure 1c. The correlation coefficient for a set of DAG–lactones with a combination of linear and branched 3-alkylidene series (**1–16**, **20–25**, **29–32**) was calculated as 0.75 as shown in Figure 1d. QSAR analysis was repeated, without log*P* values, to investigate its influence on CoMFA results. The cross-validated q^2 was dropped from 0.671 to 0.611 with 4 being the optimal number of components, and the noncross-validated r^2 was decreased correspondingly from 0.956 to 0.925. Therefore, the differences between the actual and calculated pK_i values for the training set were increased: QSAR with the CoMFA fields (standard deviation = 0.30, maximum = 0.67, and minimum = −0.54) and QSAR with the CoMFA fields and log*P* values (standard deviation = 0.23, maximum = 0.50, and minimum = −0.43). The contributions of the steric and electrostatic interaction energies and log*P* were 45.3, 38.3, and 16.4%, respectively. As expected, the steric interactions significantly contribute to the QSAR model's information, and thus explain the binding affinity variations.

The actual and calculated pK_i values for the training set are given in Table 2, and the data set is graphically represented in Figure 2. All of the compounds used in the training set have binding affinity values in the range of 2.3–6,980 nM, and the log*P* values ranged between 2.59 and 10.04. Among the DAG–lactone derivatives, compounds **8**, **13**, and **15**, which were substituted with branched 3-alkylidene chains, exhibited potent PK-Cα binding affinities, with K_i values of 2.3 and 2.9 nM. The

Table 2. Actual and calculated pK_i values for 26 molecules in the training set

Compound	K_i (nM)	pK_i	Calculated pK_i	Residual	Log*P*
1	390.00	6.41	6.44	−0.03	2.59
2	68.00	7.17	7.10	0.07	3.57
3	12.00	7.92	7.56	0.36	4.56
4	123.00	6.91	7.04	−0.13	2.68
6	5.90	8.23	8.19	0.04	4.64
7	3.50	8.46	8.29	0.17	5.62
8	2.30	8.64	8.64	0.00	6.61
9	164.00	6.79	7.18	−0.39	2.68
10	24.00	7.62	7.63	−0.01	3.66
11	7.30	8.14	8.07	0.07	4.64
13	2.90	8.54	8.48	0.06	5.89
14	8.32	8.08	8.05	0.03	4.04
15	2.90	8.54	8.04	0.50	5.03
16	6.87	8.16	8.51	−0.35	6.88
18	4330.00	5.36	5.64	−0.28	5.01
19	6980.00	5.16	5.34	−0.18	3.58
20	29.50	7.53	7.42	0.11	3.20
21	15.10	7.82	7.82	0.00	4.10
24	24.00	7.62	7.54	0.08	7.11
25	7.15	8.15	8.58	−0.43	6.72
26	605.00	6.22	6.18	0.04	7.95
27	3640.00	5.44	5.03	0.41	7.10
28	1970.00	5.71	5.84	−0.13	10.04
29	3.78	8.42	8.20	0.22	5.63
31	6.66	8.18	8.25	−0.07	5.12
32	6.88	8.16	8.30	−0.14	7.86

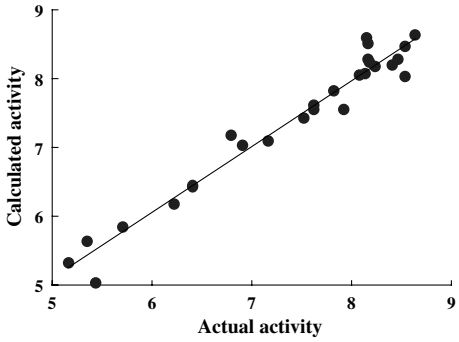

Figure 2. Actual versus calculated pK_i values for the training set.

log*P* values of compounds **8** and **13** were computed as 6.61 and 5.89, respectively, while compound **15** had a lower log*P* value (5.03). Probably, the large prediction error (0.5) for compound **15** was caused by this lower log*P* value.

The contours of the CoMFA steric and electrostatic maps are given in Figure 3. In the CoMFA steric map, the sterically favored and disfavored regions are represented in green and yellow, respectively. The large green contours surrounding the linear and branched acyl chains indicate the regions where the sterically bulky substituents enhance the biological potency, while the yellow contours show the areas where the bulky groups attenuate the potency. Remarkably, the linear 3-alkylidene chains are near the sterically unfavorable area (yellow), which explains why the longer linear alkyl chains decrease the binding affinity, as compared to the branched chains. The CoMFA electrostatic map is represented by the negatively charged favored (red) and disfavored (blue) regions. The red areas near the two carbonyls of the acyl group and the lactone ring are the regions where the functional groups with high electron densities are favorable for the PK-C activity, while the small blue areas are unfavorable. The cyclopentanone of compound **26** having lower electron density than the lactone ring is near the negatively charged favored region, which interprets the 85-fold reduction in binding affinity ($K_i = 605$ nM) by the substitution of the ester oxygen atom with a carbon ($Y = O \rightarrow CH_2$) compared to

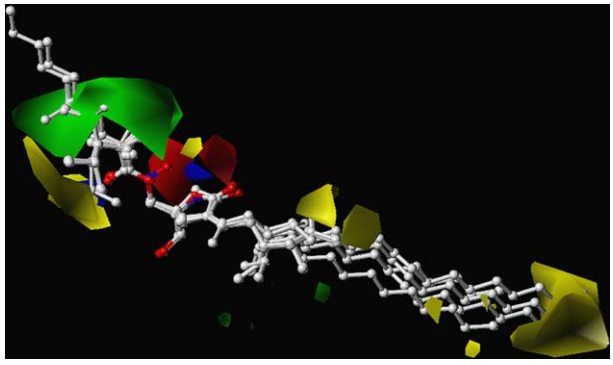

Figure 3. The contours of the CoMFA steric and electrostatic maps generated by StDev*Coeff.

Table 3. Actual and predicted pK_i values for six molecules in the test set

Compound	K_i (nM)	pK_i	Predicted pK_i	Residual	Log P
5	19.00	7.72	7.72	0.00	3.66
12	13.00	7.89	8.57	−0.68	6.61
17	429.70	6.37	5.62	0.75	3.95
22	11.00	7.96	7.75	0.21	4.10
23	35.00	7.46	7.61	−0.15	5.36
30	4.97	8.30	8.30	0.00	6.61

compound **25** ($K_i = 7.15$ nM). The investigations are quite consistent with the biological activity trends of a series of 3-alkylidene-5,5-disubstituted tetrahydro-2-furanones except for compounds **18**, **19**, **27**, and **28** displayed poor binding affinities in the training set. Although the replacement of two ester moieties of four compounds with either amide (Y = O→NH) or *N*-hydroxyl amide (X = O→N—OH) caused severe loss in the binding affinity with a range of K_i values of 1,970–6,980 nM, their molecular fields well fitted the resultant CoMFA fields. It could be explained that the ether oxygen of the lactone ring makes a hydrogen bond with the active site of PK-C C1 domain as a hydrogen-bond acceptor, while the amide N–H acts as a hydrogen-bond donor. The *N*-hydroxyl group of compound **19** might form a strong intramolecular hydrogen bond with the lactone ether oxygen, suggesting it is not directly involved in hydrogen binding with amino acids at the active site.

The predictive ability of the final 3D-QSAR model was confirmed by evaluating the experimental binding affinity values for the test set. The actual and predicted pK_i values for the test set are given in Table 3. Compound **12** produced a large prediction error (−0.68) as a test compound. Most compounds with log P values that were computed as approximately 6.5 have K_i values in the range of 2.3–7.15 nM, while compound **12** (log $P = 6.61$) showed a moderate binding affinity ($K_i = 13.0$ nM). The prediction error for compound **17** was calculated as 0.75. The ester oxygen of the acyl group in this compound was replaced by an amino group, unlike any of the other compounds in the training set. Therefore, these types of interaction fields might not be trained thoroughly in the CoMFA analysis. All of the other compounds in the test set were fairly well predicted.

3. Conclusion

The quantitative structure activity relationships (QSARs) were studied for a series of 3-alkylidene-5,5-disubstituted tetrahydro-2-furanones, developed as potent PK-C agonists, for the construction of a predictive QSAR model. The resultant QSAR model provides a significant correlation between the PK-C binding affinities (pK_i's) and the CoMFA fields, in combination with the octanol–water partition coefficient (log P). The confidence in the predictive ability of this model was confirmed by the satisfactory prediction of the experimental activities in the test set.

4. Experimental

4.1. Biological data

The binding affinity (K_i) values of DAG–lactone derivatives were used as the dependent variable (target property) in the QSAR study.[14,16–21] The molecular structures and K_i values of the 32 molecules used in the QSAR analysis are listed in Table 4. In the regression analysis, the biological activities were expressed as pK_i [$= \log(1/K_i)$]. The larger pK_i values imply higher potency for PK-C binding. Six compounds were randomly chosen for the test set. The pK_i values for all analogues ranged from 5.16 to 8.64.

4.2. Generation of three-dimensional structures of DAG–lactones

Since experimental information about the three-dimensional structures of this series is not available, the initial structure of each compound was built using the Sybyl molecular modeling program (Tripos, Inc.). The geometry was then fully optimized using the Tripos force field with the following nondefault options (method: conjugate gradient, termination: gradient 0.01 kcal/mol Å, and max iterations: 10,000). The partial atomic charges were calculated by the Gasteiger–Hückel method in the Sybyl program. The Grid search method was used to evaluate the conformational properties of all rotatable functional groups. Each torsion angle was driven from −180° to 180° in 30° increments.

4.3. Calculations of CoMFA fields and log *P* values

The calculation of the CoMFA steric and electrostatic fields requires the molecules to be superimposed in three dimensions. The alignment procedure was performed using the template structure with relatively simple methyl groups at positions R_1 and R_2, as shown in Table 4. During the alignment, all of the other molecules were fitted to the template molecule while maintaining their molecular geometry. The CoMFA steric and electrostatic interaction energies were generated using an sp^3 hybridized carbon atom as a probe with a +1.0 point charge. The energy calculation was performed with 4,320 grid points on a cube ($28 \times 30 \times 34$ Å, 2.0 Å grid spacing). The energy cutoff for the steric and electrostatic interaction energies was set to 30 kcal/mol.

The log octanol/water partition coefficients (log Ps) are frequently used to describe the lipophilic or hydrophobic

Table 4. Molecular structures and binding affinities (K_i) of DAG–lactones

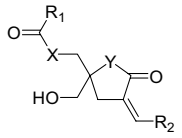

Compound	R_1	R_2	X	Y	K_i (nM)
1	CH_3	$CH{=}C(i\text{-}Pr)_2$	O	O	390.00[a]
2	$CH_3(CH_2)_2$	$CH{=}C(i\text{-}Pr)_2$	O	O	68.00[a]
3	$CH_3(CH_2)_4$	$CH{=}C(i\text{-}Pr)_2$	O	O	12.00[a]
4	CH_3	$CH_2CH(i\text{-}Pr)_2$	O	O	123.00[a]
5	$CH_3(CH_2)_2$	$CH_2CH(i\text{-}Pr)_2$	O	O	19.00[a]
6	$CH_3(CH_2)_4$	$CH_2CH(i\text{-}Pr)_2$	O	O	5.90[a]
7	$CH_3(CH_2)_6$	$CH_2CH(i\text{-}Pr)_2$	O	O	3.50[a]
8	$CH_3(CH_2)_8$	$CH_2CH(i\text{-}Pr)_2$	O	O	2.30[a]
9	$CH_2CH(i\text{-}Pr)_2$	CH_3	O	O	164.00[a]
10	$CH_2CH(i\text{-}Pr)_2$	$CH_3(CH_2)_2$	O	O	24.00[a]
11	$CH_2CH(i\text{-}Pr)_2$	$CH_3(CH_2)_4$	O	O	7.30[a]
12	$CH_2CH(i\text{-}Pr)_2$	$CH_3(CH_2)_8$	O	O	13.00[a]
13	$CH_2CH(i\text{-}Pr)_2$	$CH_2CH(i\text{-}Pr)_2$	O	O	2.90[a]
14	$(CH_3)_3C$	$CH_2CH(i\text{-}Pr)_2$	O	O	8.32[b]
15	$(CH_3)_3C$	$CH_2CH[CH_2(i\text{-}Pr)]_2$	O	O	2.90[b]
16	$CH_2CH(i\text{-}Pr)_2$	$CH_2CH[CH_2(i\text{-}Pr)]_2$	O	O	6.87[b]
17	$(CH_3)_3C$	$CH_2CH[CH_2(i\text{-}Pr)]_2$	NH	O	429.70[b]
18	$(CH_3)_3C$	$CH_2CH[CH_2(i\text{-}Pr)]_2$	O	NH	4330.00[b]
19	$(CH_3)_3C$	$CH_2CH[CH_2(i\text{-}Pr)]_2$	N—OH	O	6980.00[c]
20	$CH_2CH(i\text{-}Pr)_2$	$(CH_3)_2$	O	O	29.50[d]
21	$CH_2CH(i\text{-}Pr)_2$	$CH_2(i\text{-}Pr)$	O	O	15.10[d]
22	$CH_2(i\text{-}Pr)$	$CH_2CH(i\text{-}Pr)_2$	O	O	11.00[d]
23	CH_3	$CH_3(CH_2)_{12}$	O	O	35.00[e]
24	CH_3	$CH_3(CH_2)_7CH{=}CH(CH_2)_7$	O	O	24.00[e]
25	$(CH_3)_3C$	$CH_3(CH_2)_{12}$	O	O	7.15[f]
26	$(CH_3)_3C$	$CH_3(CH_2)_{12}$	O	CH_2	605.00[f]
27	CH_3	$CH_3(CH_2)_7CH{=}CH(CH_2)_7$	O	NH	3640.00[f]
28	$CH_3(CH_2)_6$	$CH_3(CH_2)_7CH{=}CH(CH_2)_7$	O	NH	1970.00[f]
29	$CH_3(CH_2)_4$	$CH_2CH[CH_2(i\text{-}Pr)]_2$	O	O	3.78[21]
30	$CH_3(CH_2)_6$	$CH_2CH[CH_2(i\text{-}Pr)]_2$	O	O	4.97[21]
31	C_6H_5	$CH_2CH[CH_2(i\text{-}Pr)]_2$	O	O	6.66[21]
32	$CH_2CH[CH_2(i\text{-}Pr)]_2$	$CH_2CH[CH_2(i\text{-}Pr)]_2$	O	O	6.88[21]

[a] Ref. 14.
[b] Ref. 16.
[c] Ref. 17.
[d] Ref. 18.
[e] Ref. 19.
[f] Ref. 20.

properties of chemical compounds. The log *P* values were computed using the LogKow (KowWin) program, which is based on the atom/fragment contribution method, and are shown in Tables 2 and 3.[22]

4.4. Partial least squares (PLS) analysis

To apply a multivariate data classification to the CoMFA models, a partial least square (PLS) analysis was performed using the QSAR module implemented in Sybyl. In the PLS analysis, the QSAR data sets consist of variables with different data ranges. Consequently, prior to the regression analysis, the variables are usually scaled in order to give equal influence on the outcome of the PLS analysis. In this study, the CoMFA steric and electrostatic fields and the log *P* values were scaled using the CoMFA standard scaling option. To determine the predictive q^2 and the optimum number of components for the training set, cross-validations were carried out by the 'leave-one-out' procedure. The optimum number of components corresponds to the smallest standard error of prediction. The final 3D-QSAR model was derived by a conventional analysis (noncross-validation) with the optimum number of components. All computational work was done on a Silicon Graphics O_2 R10000 workstation.

Acknowledgement

This work was supported by the Korea Research Foundation Grant (KRF-2003-015-E00229).

References and notes

1. Takai, Y.; Kishimoto, A.; Inoue, M.; Nishizuka, Y. *J. Biol. Chem.* **1977**, *252*, 7603.

2. Inoue, M.; Kishimoto, A.; Takai, Y.; Nishizuka, Y. *J. Biol. Chem.* **1977**, *252*, 7610.
3. Nishizuka, Y. *Cancer* **1989**, *63*, 1892.
4. *Protein Kinase C. Current Concepts and Future Perspectives*; Lester, D. S., Epand, R. M., Eds.; Ellis Horwood: New York, 1992.
5. *Protein Kinase C*; Kuo, J. F., Ed.; Oxford University Press: New York, 1994.
6. Livneh, E.; Fishman, D. D. *Eur. J. Biochem.* **1997**, *248*, 1.
7. Ashendel, C. L. *Biochim. Biophys. Acta* **1985**, *822*, 219.
8. Nishizuka, Y. *Science* **1992**, *258*, 607.
9. Newton, A. C. *Curr. Opin. Cell. Biol.* **1997**, *9*, 161.
10. Rando, R. R. *FASEB J.* **1988**, *2*, 2348.
11. Konig, B.; Dinitto, P. A.; Blumberg, P. M. *J. Cell. Physiol.* **1985**, *29*, 37.
12. Marquez, V. E.; Nacro, K.; Benzaria, S.; Lee, J.; Sharma, R.; Teng, K.; Milne, G. W. A.; Bienfait, B.; Wang, S.; Lewin, N. E.; Blumberg, P. M. *Pharmacol. Ther.* **1999**, *82*, 251.
13. Marquez, V. E.; Blumberg, P. M. *Acc. Chem. Res.* **2003**, *36*, 434.
14. Nacro, K.; Bienfait, B.; Lee, J.; Han, K.-C.; Kang, J.-H.; Benzaria, S.; Lewin, N. E.; Bhattacharyya, D. K.; Blumberg, P. M.; Marquez, V. E. *J. Med. Chem.* **2000**, *43*, 921.
15. PLS—Partial Least-Squares Projections to Latent Structures. In *3D QSAR in Drug Design. Theory, Methods and Applications*; Wold, S., Johansson, E., Cocchi, M., Kubinyi, H., Eds.; Escom: Leiden, 1993.
16. Lee, J.; Han, K.-C.; Kang, J.-H.; Pearce, L. L.; Lewin, N. E.; Yan, S.; Benzaria, S.; Nicklaus, M. C.; Blumberg, P. M.; Marquez, V. E. *J. Med. Chem.* **2001**, *44*, 4309.
17. Choi, Y.; Kang, J.-H.; Lewin, N. E.; Blumberg, P. M.; Lee, J.; Marquez, V. E. *J. Med. Chem.* **2003**, *46*, 2790.
18. Sigano, D. M.; Peach, M. L.; Nacro, K.; Choi, Y.; Lewin, N. E.; Nicklaus, M. C.; Blumberg, P. M.; Marquez, V. E. *J. Med. Chem.* **2003**, *46*, 1571.
19. Sharma, R.; Lee, J.; Wang, S.; Milne, G. W. A.; Lewin, N. E.; Blumberg, P. M.; Marquez, V. E. *J. Med. Chem.* **1996**, *39*, 19.
20. Kang, J.-H.; Chung, H.-E.; Kim, S. Y.; Kim, Y.; Lee, J.; Lewin, N. E.; Pearce, L. V.; Blumberg, P. M.; Marquez, V. E. *Bioorg. Med. Chem.* **2003**, *11*, 2529.
21. The binding affinities of the target compounds (**29**, **30**, **31**, and **32**) were assessed in terms of the ability of the ligand to displace bound [20-^{3}H]phorbol 12,13-dibutyrate (PDBU) from the recombinant single isozyme, PK-Cα, in the presence of phosphatidylserine as previously described.[14] The inhibition curves obtained for all ligands were of the type expected for competitive inhibition, and the IC_{50} values were determined by fitting the data points to the theoretical noncooperative competition curve. The K_i values for inhibition of binding were calculated from the corresponding IC_{50} values (Table 4).
22. Meylan, W. M.; Howard, P. H. *J. Pharm. Sci.* **1995**, *84*, 83.